

Rotational Dynamics of Vortices in Confined Bose-Einstein Condensates

S. A. McGee and M. J. Holland

JILA and Department of Physics, University of Colorado, Boulder CO 80309-0440, USA.

(March 21, 2022)

We derive the frequency of precession and conditions for stability for a quantized vortex in a single-component and a two-component Bose-Einstein condensate. The frequency of precession is proportional to the gradient of the free energy with respect to displacement of the vortex core. In a two-component system, it is possible to achieve a local minimum in the free energy at the center of the trap. The presence of such a minimum implies the existence of a region of energetic stability where the vortex cannot escape and where one may be able to generate a persistent current.

I. INTRODUCTION

Ever since Bose-Einstein condensation was first observed in a dilute atomic gas [1], considerable attention has been devoted to understanding its rotational properties. Numerous connections have already been made between superfluid phenomena in the weakly interacting atomic gases and superfluid phenomena observed in condensed matter systems (e.g. [2]). Recent demonstrations of the ability to create and observe singly quantized vortices [3,4], and vortex arrays [5], have opened up the possibility for investigations of vortex dynamics. Vortex dynamics in this context refers to the motion of topological defects within the superfluid.

A quantized vortex is represented by a singularity in a superfluid order parameter. Since the order parameter must be single-valued, the condition for quantized circulation derives from the fact that the superfluid phase ϕ must undergo a $2\pi l$ change around any closed contour, where l is an integer. Consequently, the velocity field in a superfluid is irrotational everywhere except at a vortex defect or singularity. The density at the defect is zero so that the current density vanishes even though the superfluid velocity \mathbf{v} at that coordinate is infinite. The superfluid velocity is found from the gradient of the phase by $\mathbf{v} = (\hbar/m)\nabla\phi$, where m is the mass [6]. The vortex core is the region around the defect in which the density falls from its asymptotic value to zero. The spatial scale for the core is characterized by the “healing” length $\zeta = (8\pi\rho a)^{-1/2}$, where ρ is the local superfluid number density and a is the s -wave scattering length characterizing the interactions.

It is anticipated that experimental observations on vortex dynamics [7,8] in dilute atomic Bose-Einstein condensates should agree quantitatively with predictions of the mean-field theory. External parameters such as the trap properties and the density and composition of the cloud can typically be controlled with a high degree of precision. The positions of vortex cores can be directly observed by imaging techniques rather than indirectly inferred. These features, along with possibility for multiple condensate components to be simultaneously present, make the dilute gas experiments ideal candidates for studies of vortex dynamics.

In this paper, we derive analytic solutions of the equa-

tions of motion for vortices with unit angular momentum and make comparison with full numerical simulations. The paper is outlined as follows. We begin by examining in detail a model system composed of a straight line vortex in a uniform density single-component superfluid which is confined in an infinite cylindrical vessel. Analytic solutions are presented for this well-known system for the motion of the vortex defect and connections are made with numerical calculations of the free energy. We extend these results to consider the implications of a harmonic confining potential with the associated quadratic Thomas-Fermi density envelope.

Analysis of such model systems allows us to elucidate the systematic method for generalization to more complicated systems in which analytic solutions are not easily tractable. In particular we investigate numerically the two-component condensate (relevant to current experiments at JILA for example) in which the effects of “buoyancy” must be considered. Buoyancy in this context is used to refer descriptively to a net mean-field force on a constituent of a multi-component condensate due to the various interspecies and intraspecies interaction parameters.

II. MEAN-FIELD THEORY

For a single-component condensate, we derive the motion of the vortex defect by solving the evolution of the superfluid order parameter $\Phi(\mathbf{r})$ according to the Gross-Pitaevskii equation

$$i\hbar\frac{d\Phi(\mathbf{r})}{dt} = \left(-\frac{\hbar^2}{2m}\nabla^2 + V(\mathbf{r}) + g|\Phi(\mathbf{r})|^2\right)\Phi(\mathbf{r}) \quad (1)$$

where $V(\mathbf{r})$ is the external potential and $g = 4\pi\hbar^2 a/m$. The initial condition is found by evaluating the lowest energy solution to the time-independent form of the Gross-Pitaevskii equation consistent with a given total number of atoms and a given position of the vortex defect. This requires minimizing the free energy E where

$$E = \int d^3\mathbf{r} \left(\frac{\hbar^2}{2m} |\nabla\Phi(\mathbf{r})|^2 + V(\mathbf{r})|\Phi(\mathbf{r})|^2 + \frac{g}{2} |\Phi(\mathbf{r})|^4 \right) \quad (2)$$

with the imposed constraints.

In the case of a two-component condensate, these equations are modified to account for the fact that the order parameter is a spinor $(\Phi_1(\mathbf{r}), \Phi_2(\mathbf{r}))$. The free energy is then given by

$$E = \int d^3\mathbf{r} \left(\frac{\hbar^2}{2m} (|\nabla\Phi_1(\mathbf{r})|^2 + |\nabla\Phi_2(\mathbf{r})|^2) + V_1(\mathbf{r})|\Phi_1(\mathbf{r})|^2 + V_2(\mathbf{r})|\Phi_2(\mathbf{r})|^2 + \frac{g_{11}}{2}|\Phi_1(\mathbf{r})|^4 + g_{12}|\Phi_1(\mathbf{r})\Phi_2(\mathbf{r})|^2 + \frac{g_{22}}{2}|\Phi_2(\mathbf{r})|^4 \right) \quad (3)$$

In the case of ^{87}Rb , which we will focus on here, the relevant matrix elements which characterize the interspecies and intraspecies interactions of the condensates in the applicable hyperfine states have similar values as indicated by the relationships $g_{11} = 0.97g_{12}$ and $g_{22} = 1.03g_{12}$.

For both the single-component case and the two-component case, we minimize the free energy using a steepest descents algorithm [9]. This involves propagating the Gross-Pitaevskii equation in imaginary time (by making the simple substitution $t \rightarrow -it$), and adjusting the order parameter at each step in the propagation to account for the imposed constraints. The algorithm is straightforward to implement and converges efficiently on the self-consistent lowest energy solution.

The constraints we impose depend on the symmetry of the state we wish to investigate. Since the imaginary time propagation does not preserve normalization, after each numerical step it is necessary to renormalize the order parameter to give the correct total number of atoms N . For a single-component condensate, the condition is $N = \int d^3\mathbf{r} |\Phi(\mathbf{r})|^2$. Placing the vortex defect at a given location is implemented by imposing a phase pattern about the chosen point. A single unit of circulation requires a 2π phase wrap in the order parameter. We therefore enforce that at each numerical step the order parameter has a complex phase argument of $\exp(i\theta)$ about the vortex defect, where θ is the usual counter-clockwise angle measured in the plane perpendicular to the vortex line.

For a two-component condensate the method used is similar. Given a proportion p of atoms in the first condensate component, the normalization constraints are $Np = \int d^3\mathbf{r} |\Phi_1(\mathbf{r})|^2$ and $N(1-p) = \int d^3\mathbf{r} |\Phi_2(\mathbf{r})|^2$. We adopt the convention that the component 2 is the state which will contain the single vortex line, while component 1 will contain no vortices and will therefore tend to fill the vortex core of component 1 to plug the hole in the density. In order to approximate this situation using the method of steepest descents, we enforce that the phase of $\Phi_1(\mathbf{r})$ is spatially uniform at each numerical step. The phase of component 2 is fixed at each numerical step to give a 2π phase winding around the chosen position of the defect in the same manner described for a single-component condensate.

For simplicity, we take the system to be translationally invariant along the dimension parallel to the vortex line. This allows us to solve the Gross-Pitaevskii equa-

tion in two dimensions rather than in three dimensions. To allow for comparison with experiment, the number of atoms per unit length in the two-dimensional Gross-Pitaevskii equation should take the value which reproduces the same chemical potential as the equivalent total number of atoms in the real three-dimensional system.

III. SINGLE-COMPONENT CONDENSATE

We begin our conceptual treatment of vortex dynamics in model systems with simple cases involving the motion of a quantized vortex line in a cylinder.

A. Uniform Density Distribution

Consider a uniform density superfluid confined in an infinite cylindrical vessel of radius R . A vortex is placed in the superfluid with the vortex line displaced from the cylinder axis by \mathbf{r}_0 . We define the circulation κ in the usual way to have magnitude $2\pi\hbar/m$ and to be aligned parallel to the vortex line with direction determined according to the usual right-hand rule applied to the superfluid flow. The velocity field can be found using an image vortex argument [10]. The effect of the boundary conditions at the cylinder walls is to require that the perpendicular component of the superfluid velocity is zero at the surface. This condition is satisfied by considering a formally equivalent situation of a uniform fluid of infinite extent with an additional image vortex of opposite circulation placed at $\mathbf{r}_1 = (R/r_0)^2 \mathbf{r}_0$. The velocity field for this situation is:

$$\mathbf{v}(\mathbf{r}) = \frac{\kappa}{2\pi} \times \left(\frac{\mathbf{r} - \mathbf{r}_0}{|\mathbf{r} - \mathbf{r}_0|^2} - \frac{\mathbf{r} - \mathbf{r}_1}{|\mathbf{r} - \mathbf{r}_1|^2} \right). \quad (4)$$

The motion of the vortex defect at \mathbf{r}_0 is found by computing the superfluid flow at that coordinate, which is due solely to the image vortex contribution:

$$\mathbf{v}(\mathbf{r}_0) = \frac{\kappa \times \mathbf{r}_0}{2\pi(R^2 - r_0^2)} \quad (5)$$

The angular frequency of precession of the vortex defect about the center axis of the cylinder is therefore given by $\omega = \kappa/2\pi(R^2 - r_0^2)$. Note that the angular precession direction is always in the same sense as the circulation.

An alternative approach (but equivalent method) for finding the rate and direction of precession of the vortex defect is to compute the free energy due to the attractive interaction between the real vortex and the image vortex. Ignoring the kinetic energy within the core of the vortex line, the free energy per unit length is given by [10]

$$E = \frac{\rho\kappa^2 m}{4\pi} \log \left[\frac{R^2 - r_0^2}{R\zeta} \right] \quad (6)$$

The defect velocity \mathbf{v} is then found from the solution of

$$\rho m(\boldsymbol{\kappa} \times \mathbf{v}) = \nabla E \quad (7)$$

where ∇E is the gradient of the free energy with respect to the location of the defect, i.e. \mathbf{r}_0 . The importance of this alternative approach is that, for a complex system, the free energy surface E can be calculated numerically. Consequently, the implication is that one may find the gradient of the free energy with respect to displacement of the defect as a model to infer the behavior of the vortex dynamics even when a simple analytic expression such as Eq. (6) cannot easily be derived.

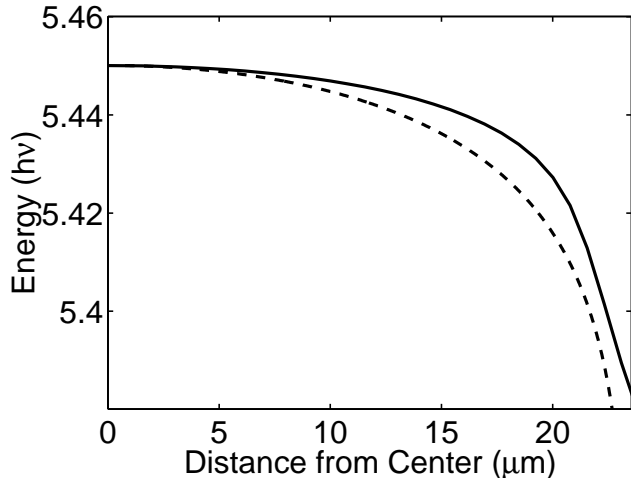


FIG. 1. Comparison of the approximate analytic expression for the free energy given in Eq. (6) (dashed line), which ignores the kinetic energy associated with the core, with the exact free energy found from the numerical solution to the Gross-Pitaevskii equations (solid line) as the amount of displacement r_0 is varied. Parameters used were $\nu = 7.8$ Hz (for convenience for comparison with later figures), $N = 4 \times 10^5$, $a = 100a_0$ where a_0 denotes the Bohr radius, m is the mass of ^{87}Rb , and $R = 23.5 \mu\text{m}$.

In order to illustrate this point, in Fig. 1 we show the results of a numerical solution of the free energy for a displaced vortex in a cylinder. The external potential $V(\mathbf{r})$ for this case changes abruptly from zero inside the cylinder to infinity at the walls. The resulting superfluid density is approximately uniform except within a small distance of the surfaces as characterized by the healing length. The exact numerical results are compared with the approximate analytic free energy expression given in Eq. (6). According to the analytic expression, the free energy diverges at the edge of the cloud, since the boundary effects associated with the core size have not been taken into account. Apart from edge effects, the analytic expression for the free energy agrees very well with the total energy found from the numerical solution of the free energy.

At zero temperature there is no energy dissipation and the motion of the vortex defect is along an equipotential of the free energy, which is circular in this case. However,

in the presence of dissipation, the defect propagates to regions of lower free energy. The vortex and image vortex attract each other in the uniform fluid since they have the opposite sign for the circulation. Consequently, for the situation considered in Fig. 1 the vortex will spiral out and eventually annihilate with the image vortex at the surface of the cylinder. At finite temperature, dissipation is generated by collisions between superfluid atoms and atoms from the non-condensed component of the cloud.

B. Thomas-Fermi Density Distribution

We now replace the superfluid of uniform density by the quadratic Thomas-Fermi density envelope. This is a good approximation to the density distribution which results from a harmonic confining potential and allows us to make contact with an experimentally more relevant situation for dilute atomic Bose-Einstein condensates. For this distribution, the density falls to zero at the Thomas-Fermi radius R in a smooth and continuous manner so the importance of edge effects is reduced.

The free energy surface results from the velocity field associated with the minimum energy configuration at each value of the radial core displacement and this may be calculated analytically in a hydrodynamic approach [6,11]. This approach is in the same spirit as the method used for the derivation of the free energy in Eq. (6) in that the kinetic energy associated with the core region, and the spatial dependence of the trapping potential and mean-field potential across the vortex core are neglected. Taking into account the Thomas-Fermi density distribution in this way gives the free energy expression

$$E = \frac{\rho_0 \kappa^2 m}{8\pi} \left[\frac{R^2 - r_0^2}{R^2} \ln \frac{R^2}{\zeta_0^2} + \left(\frac{R^2}{r_0^2} + 1 - \frac{2r_0^2}{R^2} \right) \ln \frac{R^2 - r_0^2}{R^2} \right] \quad (8)$$

where ρ_0 is the number density of the gas at the center of the trap, and ζ_0 is the corresponding healing length.

According to the implication that the gradient of the free energy surface is related to the precession frequency as given in Eq. (7), one may calculate the precession frequency within the approximations associated with Eq. (8) as [11]

$$\omega = \frac{\kappa}{4\pi(R^2 - r_0^2)} \left(2 \ln \frac{R}{\zeta_0} + \left(\frac{R^4}{r_0^4} + 2 \right) \ln \frac{R^2 - r_0^2}{R^2} + \frac{R^2}{r_0^2} + 2 \right) \quad (9)$$

Note that the precession direction for this case is always in the same sense as the circulation, so that the qualitative behavior of the motion of the vortex defect is similar to that of the uniform fluid in a cylinder.

In Fig. 2 we compare the analytic expression for the free energy given in Eq. (8) with the exact numerical solution for the free energy. The agreement is remarkable and the role of edge effects is small on the free energy and consequently on the precession frequency. The sign of the free energy gradient indicates that in the presence of dissipation, the vortex is not energetically stable and will spiral outwards to the edge of the cloud where it will disappear.

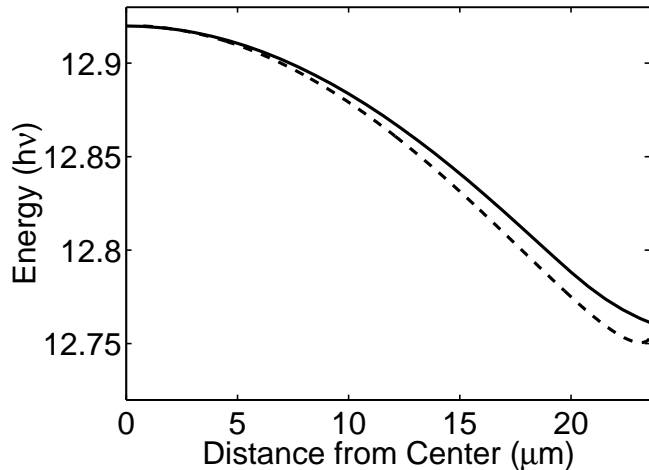


FIG. 2. Comparison of the exact numerical solution (solid line) for the free energy for the case of a Thomas-Fermi density distribution in the condensate with the analytic result derived in the hydrodynamic approximation given in Eq. (8) (dashed line) as the amount of displacement r_0 is varied. The energy falls off more gradually than for the previously considered case of a uniform fluid in a cylinder and there is no divergence of the analytic result at the boundary. The values of N , a , m , and ν are given in Fig. 1, with ν denoting in this case the frequency of the harmonic potential.

IV. TWO-COMPONENT CONDENSATE

When multiple-components are simultaneously present in a trap, the interactions are characterized by a matrix of the interspecies and intraspecies collisions. Depending on the elements of the scattering matrix, various distinct kinds of behavior are possible for the density distribution of the components.

Condensate experiments on ^{87}Rb can typically trap two-components simultaneously which tend to phase separate and are approximately immiscible in a non-uniform confining potential. In addition, within the mean-field approximation, the lowest energy solution has the component with the smaller self-interaction scattering length in regions of highest density. If this component is displaced it will tend to float to the center of the trap, where in a harmonic potential the density is greatest. A pictorial analogy is often made between this physical

mechanism and a buoyancy force in a fluid of varying density.

In terms of the implications for the vortex dynamics, the inclusion of this second component can be important even if the second component contains no vortex lines itself. The extra degree of freedom associated with the buoyancy behavior allows a more complex structure for the free energy surface.

In Fig. 3 we calculate the free energy for the case of 10^6 total ^{87}Rb atoms in the condensate in an isotropic 7.8 Hz trap with about 40% in component 1 and 60% in component 2. The scattering parameter used is $g_{12} = 4\pi\hbar^2(100a_0)/m$ where a_0 is the Bohr radius. As mentioned previously the simulation is actually performed in two-dimensions with a number of particles per unit length set to give the same chemical potential as for the three dimensional system.

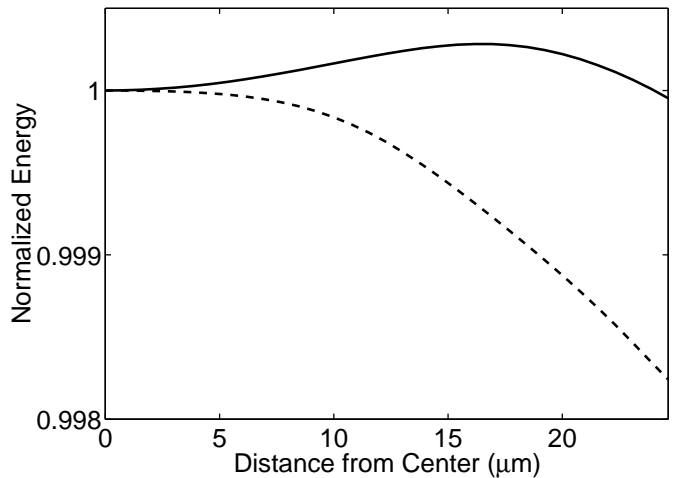


FIG. 3. Free energy for a two-component condensate as a ratio of the free energy when the defect is at the trap center. About 40% of the atoms are in component 1 (the component containing no vortices) with the rest in component 2 (the component containing a single vortex line). The solid line is for 10^6 total atoms and the dashed line is for 4×10^5 total atoms. With 10^6 total atoms there is a minimum in the free energy at the trap center, and therefore an inner region of energetic stability. However, with 4×10^5 total atoms, the mean-field effects are insufficient to generate the barrier.

The characteristic of a local minimum in the free energy at the center of the trap has significant implications. The minimum implies a critical radius R_c , which is the radius corresponding to the maximum in the free energy curve. If the displacement of the vortex line is less than R_c , the vortex will dissipate energy by spiraling inwards to the center of the trap, where it will remain forever. There is no energetic path by which the vortex can propagate to a region of zero density and annihilate. Due to its non-trivial topological structure, annihilation with a vortex of opposite circulation is required to re-

move a vortex line and this can happen trivially only in a zero-density region. Consequently, this two-component condensate system studied here can support a persistent current which is metastable, provided the vortex line is generated near the trap center. In reality, inelastic processes which have not been included in our discussion and which result from spin-exchange collisions will limit the lifetime of the metastable state.

The complementary situation exists for a vortex line which is created with a displacement larger than R_c . In the presence of dissipation, such a vortex will spiral out of the system and annihilate at the surface. If the vortex line is displaced from the trap center by exactly R_c , the forces acting on the vortex defect balance precisely, and the velocity of the singularity in the superfluid flow is zero.

These phenomena require a sufficiently strong influence of the mean-field interactions. If the total number of atoms is reduced from 10^6 to 4×10^5 with the same fraction in the non-rotating component, there is no longer a barrier in the free energy, and the critical radius is zero. In this case no energetically stable persistent currents are possible.

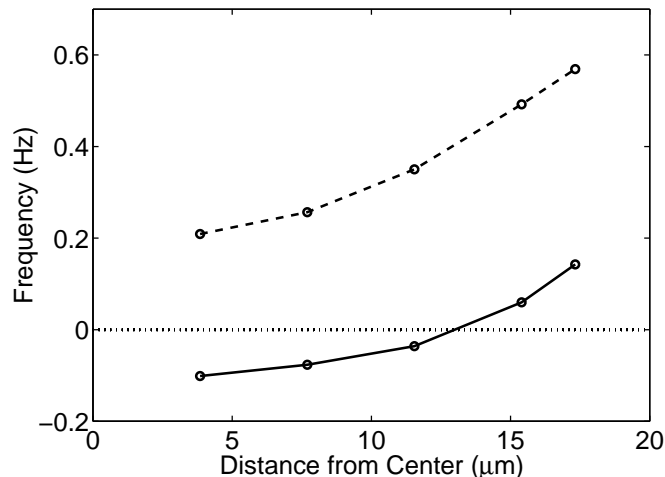


FIG. 4. The precession frequency as a function of displacement of the defect for the two cases in Fig 3. In the region where the gradient of the free energy points away from the center of the trap, the precession is in the opposite sense (clockwise) to the sense of the vortex fluid flow (counterclockwise). Where the gradient of the free energy points towards the center of the trap, the precession is in the same sense as the vortex fluid flow.

The presence of a barrier in the free energy alters qualitatively the behavior of the vortex dynamics. As illustrated in Fig. 4, when the gradient of the free energy changes sign with respect to displacement of the vortex core, so does the direction of precession of the defect, as implied by Eq. (7). Consequently, in a two-component system, the non-rotating component can modify the rate

and direction of precession of the core purely through its influence through the mean-field potential.

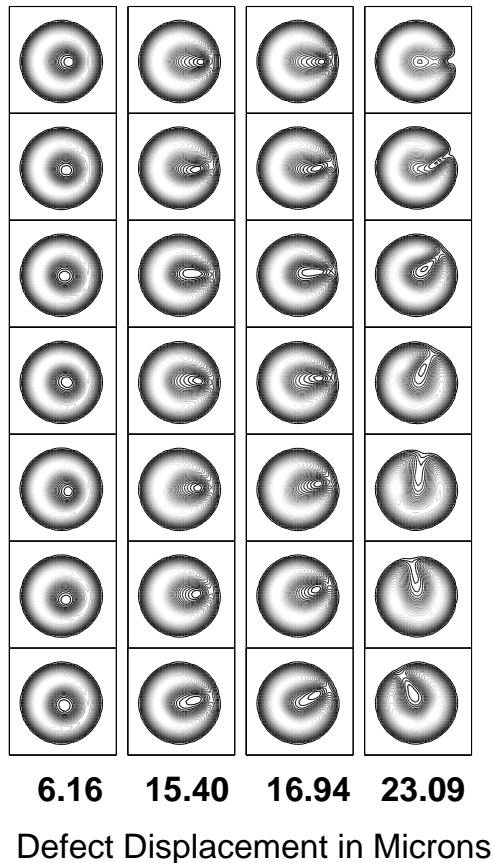


FIG. 5. Snapshots of the real-time precession of the defect for the case of 10^6 total atoms in a two-component condensate with approximately 40% in the non-rotating component. Each column represents a time evolution from top to bottom with 100 ms between each snapshot. The intrinsic superfluid circulation around the defect has been chosen to be counterclockwise for all images. The initial densities (top row) correspond to different displacements of the vortex defect from the trap center. For the smallest displacement (left column), the motion of the vortex defect is a clockwise precession while the others are precessing counterclockwise. This is due to the fact that only the first column corresponds to a displacement of the vortex defect less than the critical radius given by the barrier in the free energy for these parameters.

In Fig. 5 we illustrate density snapshots showing real-time images of the vortex dynamics for the case of 10^6 total atoms. The vortex defect in the first column, which has a displacement less than the critical radius, is precessing clockwise, opposite to the chosen direction of the superfluid circulation. The others are precessing counterclockwise, which is the same sense as the intrinsic vortex fluid flow. For each of these columns, the rate of precession is in accordance with the gradient of the of the free energy curve calculated numerically for the same param-

eters. In Fig. 6 similar snapshots are shown for the case for 4×10^5 total atoms. Here, the defect is precessing counterclockwise at all displacements, and the barrier in the free energy is absent.

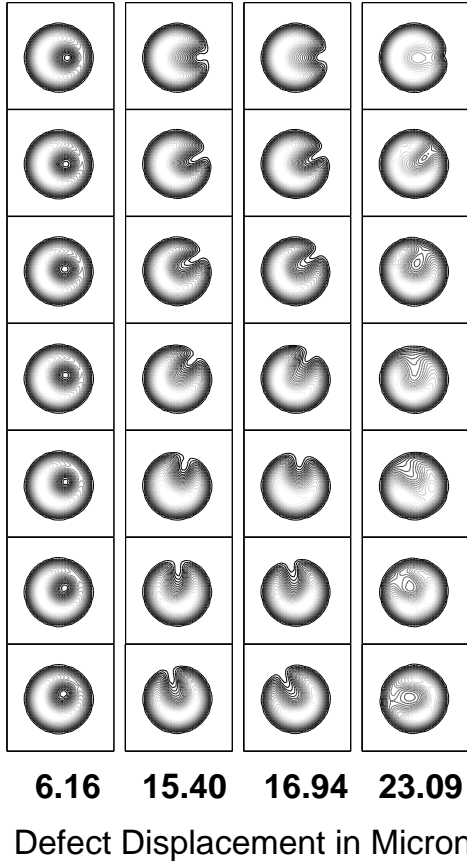


FIG. 6. Simulation of the real-time vortex dynamics as in Fig. (5) with the same fraction of 40% in the non-rotating component, but illustrating the effect of reducing the total number of atoms to 4×10^5 . The motion of the vortex defect is in the same sense as the circulation of the vortex for all displacements from the center. This results from the absence of the free energy barrier due to the reduction in the mean-field buoyancy effects.

V. CONCLUSION

We have found that for a single-component condensate the precession direction will always be in the same sense as the vortex fluid flow for both the uniform density in a cylinder and for the Thomas-Fermi density profile. Such a vortex is not energetically stable, and in the presence of dissipation, will spiral out to the edge of the cloud and annihilate. Including the effects of kinetic energy in the core region and edge effects at the surface of the cylinder in the free energy gave minor modifications to the vortex dynamics from that predicted by the hydrodynamic theories.

For a two-component condensate, numerical calculations demonstrated the possibility for the precession direction to be opposite to the sense of the vortex fluid flow. In this case, the vortex will dissipate energy by spiraling to the center of the trap. Such a situation occurs whenever there is a minimum in the free energy as a function of displacement of the vortex defect. This possibility allows a metastable persistent current which may remain indefinitely, even in the presence of thermal fluctuations. This is due to the topological nature of the vortex prohibiting annihilation and is a manifestation of superfluidity. When there are insufficient atoms, the absence of an energy barrier causes the vortex to spiral outward. This case is similar to the case of a vortex in a single-component condensate, with a modified precession frequency.

VI. ACKNOWLEDGEMENTS

We would like to thank A. Fetter, E. Cornell, B. Anderson, and P. Haljan for helpful discussions. This work was supported by the National Science Foundation.

-
- [1] M. H. Anderson, J. R. Ensher, M. R. Matthews, C. E. Wieman, and E. A. Cornell, *Science* **269**, 198 (1995); C. C. Bradley, C. A. Sackett, J. J. Tollett, and R. G. Hulet, *Phys. Rev. Lett.* **75**, 1687 (1995); K. B. Davis, M.-O. Mewes, M. R. Andrews, N. J. van Druten, D. S. Durfee, D. M. Kurn, and W. Ketterle, *Phys. Rev. Lett.* **75**, 3969 (1995).
 - [2] C. Raman, M. Köhl, R. Onofrio, D. S. Durfee, C. E. Kuklewicz, Z. Hadzibabic, and W. Ketterle, *Phys. Rev. Lett.* **83**, 2502 (1999).
 - [3] J. E. Williams and M. J. Holland, *Nature* **401**, 568 (1999).
 - [4] M. R. Matthews, B. P. Anderson, P. C. Haljan, D. S. Hall, C. E. Wieman, and E. A. Cornell, *Phys. Rev. Lett.* **83**, 2498 (1999).
 - [5] K. W. Madison, F. Chevy, W. Wohlleben, J. Dalibard, *Phys. Rev. Lett.* **84**, 806 (2000).
 - [6] A. L. Fetter, *J. Low Temp. Phys.* **113**, 189 (1998).
 - [7] B. P. Anderson, P. C. Haljan, C. E. Wieman, and E. A. Cornell, *cond-mat/0005368*.
 - [8] F. Chevy, K. W. Madison, and J. Dalibard, *cond-mat/0005221*.
 - [9] J. E. Williams, Ph.D. Thesis, University of Colorado, (1999).
 - [10] G. B. Hess, *Phys. Rev.* **161**, 189 (1967).
 - [11] E. Lundh and P. Ao, *Phys. Rev. A* **61**, 63612 (2000).
 - [12] A. A. Svidzinsky and A. L. Fetter, *Phys. Rev. Lett.* **84** (to be published) (2000).
 - [13] P. A. Ruprecht, M. J. Holland, K. Burnett, and M. Edwards, *Phys. Rev. A* **51**, 4704 (1995).